



COMPILATION OF DIGITAL STRONG MOTION DATA FOR EASTERN CANADA

Lan Lin¹ and John Adams²

ABSTRACT

The Geological Survey of Canada has been recording digital earthquake ground motions in eastern Canada since 1970. Two recording digital networks are currently deployed; a strong-motion network and a weak-motion network. We have compiled the triggered digital ground motion records from the Etna instruments of the strong-motion network. Based on a detailed review of the records, 243 records obtained between 1997 and 2009 were associated with earthquakes and selected for processing. The selected records are from 27 earthquake events with magnitudes ranging from 2.5 to 5.5. To validate the recorded strong motion data, records obtained by the strong-motion network were compared with corresponding weak-motion records (i.e., from the same event at the same station). It was found that the records from these two networks are very close, which confirmed that both the strong motion and weak motion records accurately represent the ground motions.

Introduction

Records of ground motions due to earthquakes are very important for seismologists and structural engineers. They are essential for understanding the regional seismicity, the development of attenuation relations for earthquake ground motions, and for investigation of the behaviour of structures subjected to ground motions.

In the past decades, significant changes have been made to the instruments for collecting ground motion data. The older type of instruments (i.e., the analogue SMA-1 instruments and paper seismographs) have been replaced by modern digital instruments, such as IA (i.e., internet-accelerometer), Etna, and digital seismometers.

In eastern Canada, there are two ground-motion monitoring networks, a strong-motion network and a weak-motion network. In terms of the instruments, Etna and IA instruments are currently used in the strong-motion network, while short-period and broad-band seismometers are used in the weak-motion network. A recent description of the national strong-motion network is given by Cassidy et al. (2007), which can be found reference to earlier descriptions. The IA network has recently been described by Rosenberger et al. (2007).

¹Postdoctoral fellow, Geological Survey of Canada, Ottawa, Ontario, Canada, K1A 0Y3, llin089@gmail.com

²Seismologist, Geological Survey of Canada, Ottawa, Ontario, Canada, K1A 0Y3, jadams@nrcan.gc.ca

This paper describes the compilation of strong motion data from eastern Canada recorded by Etnas. A comparison of waveforms based on data recorded by the strong-motion network and the weak-motion network is also presented. Since the earlier strong-motion records obtained by SMA-1 instruments from Miramichi Earthquake (1982), Nahanni Earthquake (1985), and Saguenay Earthquake (1988) are described in GSC Open Files (Weichert et al. (1982); Weichert et al. (1986); Munro and North (1989)), these records are not discussed in this paper.

Strong Motion Network in Eastern Canada

Station Information

Currently, there are 33 strong motion stations with Etna instruments in eastern Canada. IA instruments are also installed at some of these stations. All the stations are operated by Geological Survey of Canada (GSC). Figure 1 shows the current GSC Etna stations. Most of the stations are located in Charlevoix region, Québec, and were installed to capture the next strong earthquake in this seismically active region including ground motions into New Brunswick. Seven stations (i.e., OTBB, OT001, OTGH, OTNM, OTRS, OTT, and OTWM) are located in Ottawa, Ontario to assess ground motion amplification on soft soil (Adams, 2007). Station JBQQ (see Fig. 1), which is on the north-west of Ottawa, is near the location of the 1935 M_w 6.2 and 2000 M_w 4.7 Timiskaming earthquakes. The distribution of the instruments is based on the seismicity of the region.

Table 1 provides detailed information for the GSC's strong-motion stations in eastern Canada, such as station code, installation date, coordinates of stations, instrument housing (i.e., on free field or in basement of buildings), and soil condition of the stations. As seen in the table, 13 instruments are installed on free field, and 20 are in the basement of 1 or 2-storey buildings which is believed to be approximate for free field. In terms of soil conditions, 7 stations (mostly in the Ottawa region) are on soft soil while the remaining 26 stations are on bedrock.

Characteristics of Instruments

The basic characteristics of the Etna and the IA instruments are the same for all the instruments of the eastern strong-motion network. Some of them which are needed for data processing are as follows:

- Data type: the data recorded by both the Etna and the IA instruments are accelerations.
- Number of components recorded: Each record obtained by Etna and IA instruments consists of three components of ground motions, i.e., one vertical component (V) and two orthogonal horizontal components, usually oriented in North-South (N-S) and in East-West (E-W) directions.
- Sampling rate: the sampling rate of the Etna instruments is 200 samples per second (i.e., the time interval of the recorded data is 0.005 s), while that of the IA instruments is 100 samples per second (i.e., time interval of the data is 0.01 s).

It is useful to mention that there are certain differences between the Etna and the IA

instruments being used in the eastern Canadian strong-motion network. The most significant of these are summarized below:

- (1) The maximum peak ground acceleration (PGA) that can be recorded by the IA instruments is 4g, while the maximum PGA that can be recorded by Etna instruments is 2g.
- (2) The timing accuracy of IA instruments is around ± 0.01 s since the timing system of IA is controlled by Network Time Protocol over Internet. However the timing accuracy of Etna is much less than that of IA since the clock in Etna can only be adjusted manually by technicians during their on-site visit, and may drift many seconds (or several minutes).
- (3) The Etna records triggered data (including 10 seconds of pre-event signal), while IA records continuous data.
- (4) The IA instrument is linked by internet and so can provide real-time readings while Etna must be visited by technician to recover data and cannot provide real-time readings.

Strong Motion Records

The eastern strong-motion network has provided a large number of records of earthquake ground motions between 1997 and 2009. For the purpose of processing of the records, a detailed review was conducted on all the saved triggered data. Based on this review, 81 records, i.e., 243 components ($=81*3$) were selected for processing. The selected records were obtained from 22 earthquakes that recently occurred in eastern Canada and adjacent US. The characteristics of these earthquake events are summarized in Table 2. It can be seen in the table that the Nuttli magnitudes (m_N) of the events are between 2.5 and 5.5, the moment magnitudes (M_w) are between 2.1 and 4.9. The numbers of records from each earthquake are also included in the table. Note that about 30% of the records are from the M_w 4.7 Rivière-du-Loup earthquake that occurred on March 6, 2005. This earthquake is one of the largest earthquakes that occurred recently in eastern Canada. The strong motion records from the Rivière-du-Loup earthquake, 2005/03/06/ can be found in GSC Open File 6544 (Lin and Adams, 2010).

Processing of Strong Motion Records

The recorded data are normally called "raw" or "uncorrected" data and these need to be processed in order to be useful for seismologists and structural engineers. The objective of the processing of a recorded component of a ground motion is to determine the "corrected" acceleration data, as well as the velocity and the displacement data of the ground motion. The corrected accelerations are further used to compute the response spectra and the Fourier spectra of the ground motions.

The data processing procedure depends on the type of the instrument used for the recording of ground motions. The two main phases of the data processing of a given record are the baseline correction and the filtering of the record.

The baseline correction is necessary to remove the offset of the record (i.e., the initial shift of the record from the zero line) that might be present in the record. This offset can be easily recognized based on the pre-event portion of the record.

The filtering of the record is done to remove high frequency and low frequency noise that might be present in the record. This requires the application of a band-pass filter. In general, various numerical band-pass filters can be used in the filtering of records.

For illustration, Figure 2 shows the “corrected” acceleration waveform for the N-S component obtained by processing the recorded motion at station A16 during the March 6, 2005 Rivière-du-Loup earthquake. The processing was conducted as discussed above, i.e., by applying baseline correction and filtering of the record. A band-pass Butterworth filter of the order of 4, with high-pass frequency of 0.3 Hz and low-pass frequency of 50 Hz was used in the filtering. The PGA value of this record is about 3% g.

For the purpose of obtaining reliable information from the records, Geological Survey of Canada is currently conducting: (i) comparisons of ground motion records obtained by both the strong-motion and the weak-motion networks, and (ii) investigations of various parameters that affect the processed data. An example from the comparisons of records from the strong-motion and the weak-motion networks is discussed below.

Case Study

The objective of this study is to compare the records obtained by Etna from the GSC strong-motion network with corresponding records obtained by seismometers from the weak-motion network. This study was undertaken to check the quality of the recorded data. Comparisons of the records from these two networks are needed since different types of instruments are deployed in the networks.

Records obtained during the Rivière-du-Loup earthquake on March 6, 2005 in Québec (Table 2) were considered in the case study. This event is one of the largest earthquakes occurred in recent years in eastern Canada. The records obtained at station A11 from the strong-motion network and the weak-motion network were used in the study. Among the three components, only the results for the North-South (N-S) component are presented here. The comparisons of the other components (i.e., V and E-W) provided similar results, and they are not shown in this paper.

For easier discussion, the N-S component recorded by Etna in the strong-motion network is designated HNN while the N-S component recorded by seismometer in the weak-motion network is designated HHN. This designation is consistent with the SEED channel naming convention (IRIS, 2009).

Figure 3 shows the HNN and the HHN waveforms of 2005/03/06 Rivière-du-Loup earthquake recorded at station A11 (Table 1). The two records shown in the figure are based on the **raw** data. Only two adjustments were made to the records, (1) for HNN record, the DC offset was removed, (2) for HHN record, the recorded velocity data were converted to acceleration.

Note that all processing in this study was conducted using SAC software (LLNL, 2005).

Waveforms Similarity Comparison

In order to determine the similarity of the two waveforms shown in Fig. 3, waveforms similarity analysis should be performed. Normally it can be done by considering cross correlation functions (CCF). The mathematical expression of CCF for two functions f and g is given in Eq. 1. From Eq. (1), one can determine how much g should be shifted in order to make it identical to f . In the ground motion data processing, functions f and g are normally referred to as waveforms, and the shifting of a function, for example, g , is called time-lag of waveform g relative to waveform f .

$$(f * g)[n] = \sum_{-\infty}^{\infty} f^*[m]g[n+m] \quad (1)$$

CCF results for the HNN and the HHN waveforms obtained using SAC are given in Fig. 4. It was found from the figure that the time-lag corresponding to the peak CCF value is around 52.25 seconds, i.e., the HHN waveform should be shifted 52.25 seconds in order to give the highest correlation with the HNN waveform. This time-lag results from clock drift in the Etna.

Knowing the time-lag of the HNN and the HHN waveforms, the two waveforms are superimposed to determine how similar they are. The results are shown in Fig. 5. Note that the accelerations for both HNN and HHN are plotted in g. It can be seen in Fig. 5 that the HNN and the HHN waveforms match very well. Also, the PGA values are very close, i.e., PGA of the HNN waveform is 0.0083g while that of the HHN waveform is 0.0082g. For easier comparison of the HNN waveform and the HHN waveform, the time-scale for the segment between 10 s and 15 s is enlarged (Fig. 6). This segment is selected since it represents the strong motion part of the records. It is seen in Fig. 6 that the HNN and the HHN waveforms are almost identical. Comparisons for other segments of the waveforms (i.e., 0 – 10 s, 15 – 20 s, 20 – 25 s, etc, which are not shown here) were also conducted. The observations from these comparisons are the same as those from Fig. 6. Furthermore, by regression analysis it was found that the correlation coefficient of the HNN and HHN waveforms is 0.993. This indicates that HNN and HHN are very similar.

Comparison of Fourier Spectra

In addition to the comparison of the waveforms, the Fourier amplitude spectra of the HNN and the HHN records were compared to see the similarity of the records at different frequencies. Figure 7 shows smoothed Fourier amplitude spectra for the HNN and the HHN waveforms presented in Fig. 3, and Fig. 8 shows the spectral ratio. The main findings from the figures can be summarized as follows:

- The shapes of the Fourier spectra for the HNN and the HHN records are very similar.
- The predominant frequency for both records is about 7 Hz.
- The amplitudes of the HNN and the HHN Fourier spectra are quite close (spectral ratio is about 0.99) for frequencies between 0.9 Hz and 24 Hz. The differences for the Fourier amplitudes are around 10% for frequencies above 24 Hz and below 0.9 Hz. Such

differences may indicate a problem in the calibration (instrument response) equation outside the key band of 0.9-24 Hz of the instruments.

In summary, the results from the Fourier analysis indicate that the HNN and the HHN waveforms are very similar, which is consistent with the conclusion drawn from the waveforms similarity analysis in the previous section.

The results from the case study show that the waveforms recorded by the instruments of the strong-motion network (Etnas) and those of the weak-motion network (seismometers) from the same event at the same station have a very good agreement in terms of the shape of the time-trace, PGA value, and Fourier spectrum. This also confirms the accuracy of the calibration of the instruments in both the strong-motion and the weak-motion networks.

Conclusions

A comprehensive project was undertaken by Geological Survey of Canada (GSC) with the objective to compile and process the available records from eastern Canada obtained by the strong-motion network. This paper presents an overview of the compilation of strong-motion records that is underway in GSC. Among a number of records, 243 records (raw data) obtained during the last decades were selected to load in the Canadian National Waveform Archive. Also, a case study is discussed, which was to determine the accuracy of the strong-motion records. This was done by comparing selected records obtained from the strong-motion network with those obtained from the weak-motion network. The results show that the records from these two networks are very close. This indicates that the strong-motion data are consistent with those currently available in the weak-motion database (at least for Canadian National Seismograph Network (CNSN)).

It is believed that the compiled strong-motion records will be very useful for better understanding the seismicity in eastern Canada, the updating of the attenuation relations for ground motions, and in general, for the improvement of the seismic design of structures in Canada.

Several projects that might be considered by GSC in the future include, (i) loading Etna data into Canadian National Waveform Archive to make the data accessible through the internet, (ii) processing IA data in similar fashion, (iii) assembly of digitized analog data, and (iv) collection of strong motion data in eastern Canada from other parties.

Acknowledgements

The authors thank all the GSC's staff, especially technician Scott Desjardins and computer scientist Xiuying Jin, for their efforts in managing eastern Canadian strong motion network. Thanks are also due to Dr. Allison Bent for her advice with using SAC software. Special thanks are given to Mr. Stephen Halchuk for his generous help whenever needed.

References

- Adams, J., 2007. Soil Amplification in Ottawa from Urban Strong Ground Motion Record. 9th Canadian Conference on Earthquake Engineering, Paper No. 1162, 379-389, Ottawa, ON, Canada.
- Cassidy, J.F., Rosenberger, A., Rogers, G.C., Little, T.E., Toth, J., Adams, J., Munro, P., Huffmann, S., Pierre, J.R., Asmis, H., Pernica, G., 2007. Strong Motion Seismograph Networks in Canada. 9th Canadian Conference on Earthquake Engineering, Paper No. 1310, 459-468, Ottawa, ON, Canada.
- IRIS, 2009. Standard for the exchange of earthquake data, Incorporated Research Institutions for Seismologists, Washington, United States.
- Lin, L., Adams, J. 2010. Strong motion records of the Rivière-du-Loup, Québec Earthquake of March 6, 2005. *Geological Survey of Canada Open File 6544* (in press), Ottawa, Ontario.
- LLNL, 2005. Seismic Analysis Code, Lawrence Livermore National Laboratory, Livermore, California, United States.
- Munro, P.S., and North, R.G., 1989. The Saguenay Earthquake of November 25, 1988 Strong Motion Data, *Geological Survey of Canada Open File 1976*, Ottawa, Ontario, Canada.
- Rosenberger, A., Rogers, G.C., and Cassidy, J.F., 2007. The New Real Time Reporting Strong Motion Seismograph Network in Southwest BC: More Strong Motion Instruments for less Money, 9th Canadian Conference on Earthquake Engineering, Ottawa, ON, Canada.
- Weichert, D.H., Pomeroy, P.W., Munro, P.S., and Mork, P.N., 1982. Strong Motion Records from Miramichi, New Brunswick, 1982 Aftershocks, *Earth Physics Branch Open File 82-31*, Ottawa, Ontario, Canada.
- Weichert, D.H., Wetmiller, R.J., Horner, R.B., Munro, P.S., and Mork, P.N., 1986. Strong Motion Records from the 23 December 1985, Ms6.9 Nahanni, NWT, and some associated earthquakes. *Geological Survey of Canada Open File Report 1330*, Ottawa, Ontario, Canada.

Table 1. List of GSC strong-motion stations.

No.	Station Code	Installation Date	Station Name	Coordinates	Elevation (m)	Instrument	Instrument Housing	Soil Condition
1	A11	1999/06/27	St-Roch des Aulnaies, Québec	47.2431 N 70.1968 W	76	Etna	Above ground seismic vault on bedrock	Bedrock
2	A16	1999/06/26	Rivière Ouelle, Québec	47.4680 N 70.0096 W	72	Etna	Above ground seismic vault on bedrock	Bedrock
3	A21	1999/09/25	St-André, Québec	47.7045 N 69.6891 W	66	Etna	Above ground seismic vault on bedrock	Bedrock
4	A54	1999/06/26	Misere, Québec	47.4568 N 70.4134 W	414	Etna	Above ground seismic vault on bedrock	Bedrock
5	A61	1999/06/18	Sainte-Mathilde, Québec	47.6936 N 70.0914 W	372	Etna	Above ground seismic vault on bedrock	Bedrock
6	A64	1999/06/23	Saint-Siméon, Québec	47.8274 N 69.8914 W	184	Etna	Above ground seismic vault on bedrock	Bedrock
7	BOIN	2007/06/26	Boiestown, New Brunswick	46.4628 N 66.4067 W	86	Etna	Basement, house	Bedrock
8	BSPQ	1999/02/26	Baie St-Paul, Québec	47.4418 N 70.5057 W	23	Etna	Basement, 2-storey building, City Hall	Alluvium
9	CHIQ	2000/10/06	Chicoutimi-Nord, Québec	48.4902 N 71.0123 W	133	Etna	Foundation, house	Bedrock
10	EDMN	2000/10/16	Edmundston, New Brunswick	47.4607 N 68.2398 W	186	Etna	Basement, house	Bedrock
11	JBBQ	2001/12/04	Temiscaming, Québec	46.7751 N 78.9632 W	278	Etna	Basement, house, Home of Claude Brisson	Bedrock
12	LMBQ	1999/02/26	La Malbaie, Québec	47.6555 N 70.1526 W	42	Etna	Basement, 1-storey building, Post Office	Bedrock
13	LMQ	1998/10/02	Les Eboulements, Québec	47.5485 N 70.3258 W	429	Etna	Above ground seismic vault on bedrock	Bedrock
14	MNT	1999/10/15	Montréal, Québec	45.5025 N 73.6231 W		Etna	Basement, 4-storey building, Collège Brébeuf	Bedrock
15	MRHQ	2004/10/13	Morin Heights, Québec	45.8870 N 74.2127 W	422	Etna	Above ground seismic vault on bedrock	Bedrock
16	OT001	2001/11/15	Orleans, Ontario	45.4788 N 75.4745 W	88	Etna, IA	Basement, 2-storey wood house	Clay, Silt, Silt-clay
17	OTBB	2002/05/23	Ottawa, Ontario	45.4068 N 75.5548 W	76	Ena	Basement, 1-storey wood building	Alluvium
18	OTGH	2001/12/18	Ottawa, Ontario	45.4014 N 75.6969 W	74	Ena	Basement, 4-storey masonry building, Glebe High School	Thin alluvium
19	OTNM	2003/06/11	Ottawa, Ontario	45.4121 N 75.6891 W	72	Ena	Basement, 4-storey building, Canadian Museum of Nature	Alluvium
20	OTRS	2002/05/15	Orleans, Ontario	45.4603 N 75.4962 W	90	Etna	Basement, 2-storey wood building	Alluvium
21	OTT	2002/02/27	Ottawa, Ontario	45.3942 N 75.7167 W	77	Etna, IA	Basement, 3-storey building	Bedrock
22	OTWM	2001/11/08	Ottawa, Ontario	45.3824 N 75.7628 W	69	Ena	Basement, 2-storey wood building	Alluvium
23	QCQ	1997/11/01	Québec, Québec	46.7791 N 71.2760 W	111	Etna	Basement, 3-storey building, Université Laval	Bedrock
24	RDLQ	1999/03/01	Rivière du Loup, Québec	47.8352 N 69.5376 W	55	Etna	Basement, 2-storey building, Post Office	Bedrock
25	RIMQ	2005/07/22	Rimouski, Québec	48.4449 N 68.4820 W	124	Etna	Above ground seismic vault on bedrock	Bedrock
26	ROUQ	1999/06/28	Rivière Ouelle, Québec	47.4753 N 69.9966 W	32	Etna	Basement, house	Bedrock
27	SANQ	2004/11/25	St-André du lac St-Jean, Québec	48.3249 N 71.9886 W	296	Etna	Above ground seismic vault on bedrock	Bedrock
28	SELQ	1999/09/27	St-Éléuthère, Québec	47.4958 N 69.3620 W	463	Etna	Basement, house	Bedrock
29	SFA	1999/09/30	St-Ferréole les Neiges, Québec	47.1244 N 70.8266 W	230	Etna	Under ground seismic vault, Hydro-Québec	Bedrock
30	SGRQ	1999/09/29	St-Georges, Québec	46.1399 N 70.5788 W	332	Etna	Basement, house	Bedrock
31	SLBQ	1999/09/28	St-Lucie de Beauregard, Québec	46.7418 N 70.0160 W	410	Etna	Above ground seismic vault, Private Garage	Bedrock
32	STPQ	1999/03/01	St-Pascal, Québec	47.5262 N 69.8049 W	62	Etna	Basement, 1-storey building, Post Office	Bedrock
33	TADQ	1999/02/27	Tadoussac, Québec	48.1437 N 69.7184 W	46	Etna	Basement, 1-storey building, Post Office	Bedrock

Table 2. List of earthquakes recorded by Etna instruments.

No.	Event	Location	Date	Magnitude		Depth (km)	Number of records	Closest record (km)
				m_N	M_w			
1	Rivière-du-Loup	47.75 N 69.73 W	20050306	5.4	4.7	13.3	66	6
2	Cap-Rouge	46.80 N 71.42 W	19971106	5.1	4.9	22.5	3	56
6	Au Sable Forks	44.53 N 73.73 W	20020420	5.0	4.7	5.0	15	173
3	Thurso	45.65 N 75.23 W	20060225	4.5	3.9	20.0	6	36
4	Laurentide Fauna Reserve	47.56 N 71.06 W	20000712	4.2	3.8	18.0	15	42
5	Rivière-du-Loup	47.74 N 69.74 W	20081115	4.2	3.6	13.3	9	15
7	Charlevoix	47.70 N 70.09 W	20030613	4.1	3.8	10.9	15	1
8	Charlevoix	47.38 N 70.46 W	20060407	4.1	3.8	24.5	21	8
9	Charlevoix	47.33 N 70.51 W	20020817	3.8	3.4	18.0	9	16
10	Charlevoix	47.67 N 69.80 W	20000615	3.7	3.3	11.4	9	9
11	Charlevoix	47.65 N 69.92 W	20010522	3.5	3.1	11.4	6	13
12	Charlevoix	47.37N 70.31 W	20080103	3.4	3.1	13.5	6	16
13	Rogersville	46.60N 66.31 W	20090308	3.4	3.1	10.0	9	17
14	Charlevoix	47.41N 70.37 W	20070927	3.3	3.1	14.5	6	11
16	Charlevoix	47.53N 69.86 W	20031011	3.1	2.8	23.2	3	4
17	Charlevoix	47.51N 70.02 W	20020612	3.1	2.8	7.8	6	4
18	Charlevoix	47.65N 69.92 W	20010522	3.1	2.8	10.9	6	20
19	Charlevoix	47.51N 70.02 W	20020612	3.1	2.8	7.8	3	5
20	Charlevoix	47.62N 70.18 W	20061031	3.0	2.7	14.4	3	4
21	Charlevoix	47.64N 70.18 W	20040524	3.0	2.7	13.6	6	3
22	Charlevoix	47.47N 70.04 W	20000927	3.0	2.7	8.1	3	2
23	Charlevoix	47.40N 70.48 W	20011003	3.0	2.9	9.9	3	5
24	Charlevoix	47.56N 70.28 W	19981021	2.6	2.3	9.8	3	4
25	La Malbaie	47.65N 70.22 W	20041118	2.6	2.3	6.7	3	5
26	Charlevoix	47.56N 70.28 W	19981021	2.6	2.3	9.8	6	20
27	Charlevoix	47.33N 70.51 W	20020817	2.5	2.1	18.0	3	12

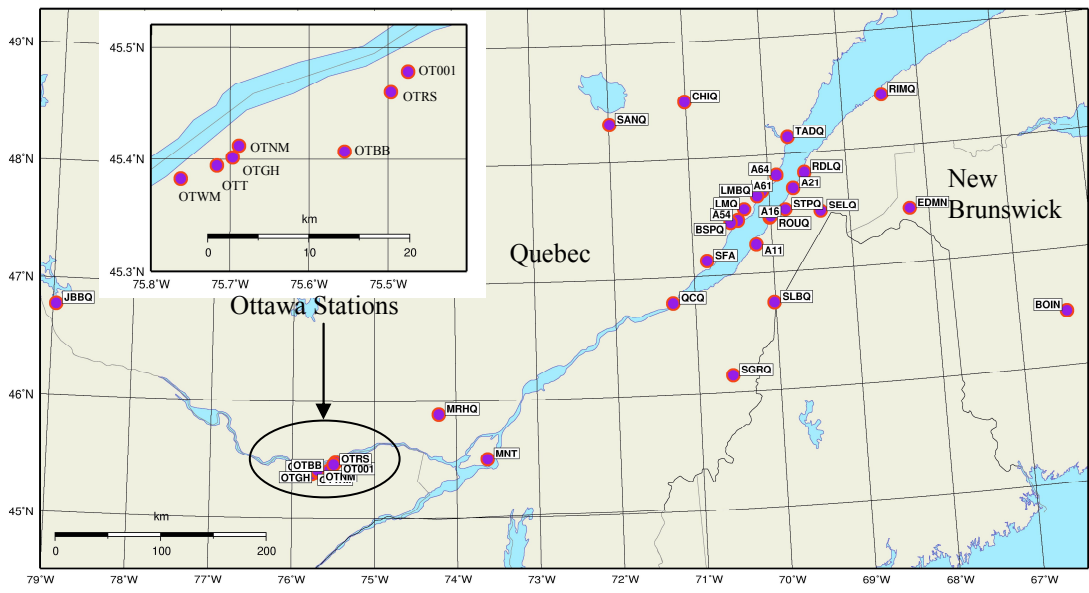


Figure 1. GSC strong-motion stations in eastern Canada, 2009.

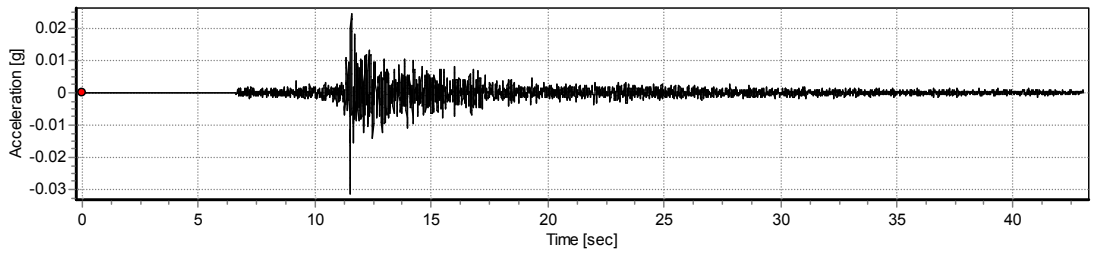


Figure 2. A sample of "corrected" acceleration waveform recorded at station A16 from 2005/03/06, Rivière-du-Loup earthquake.

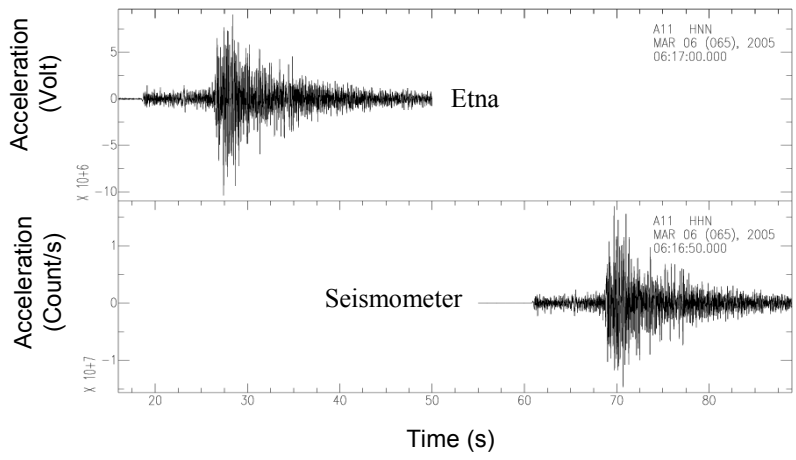


Figure 3. HNN waveform and HHN waveform for N-S component recorded at station A11 from Rivière-du-Loup earthquake.

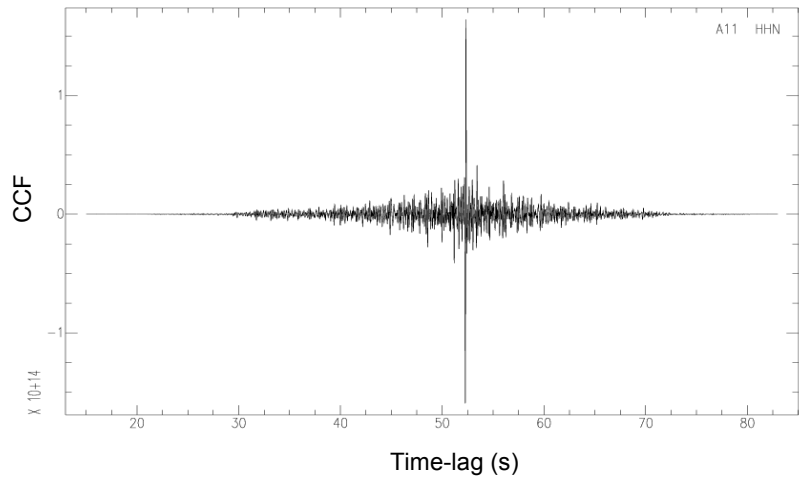


Figure 4. Cross correlation functions for HNN and HHN waveforms.

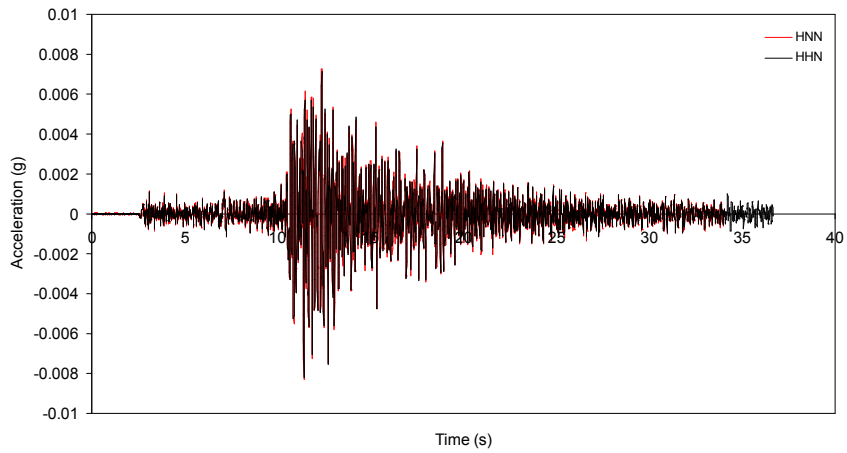


Figure 5. Comparison of HNN and HHN waveforms.

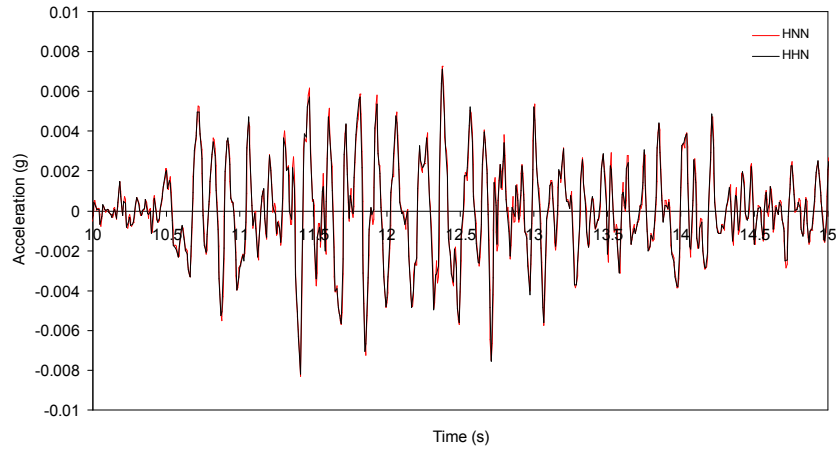


Figure 6. Comparison of HNN and HHN waveforms for the segment between 10 s and 15 s.

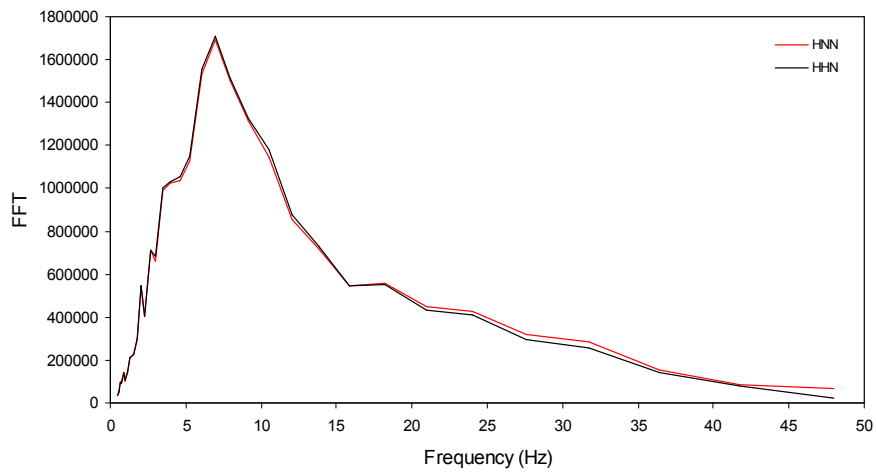


Figure 7. Fourier spectra for HNN and HHN data.

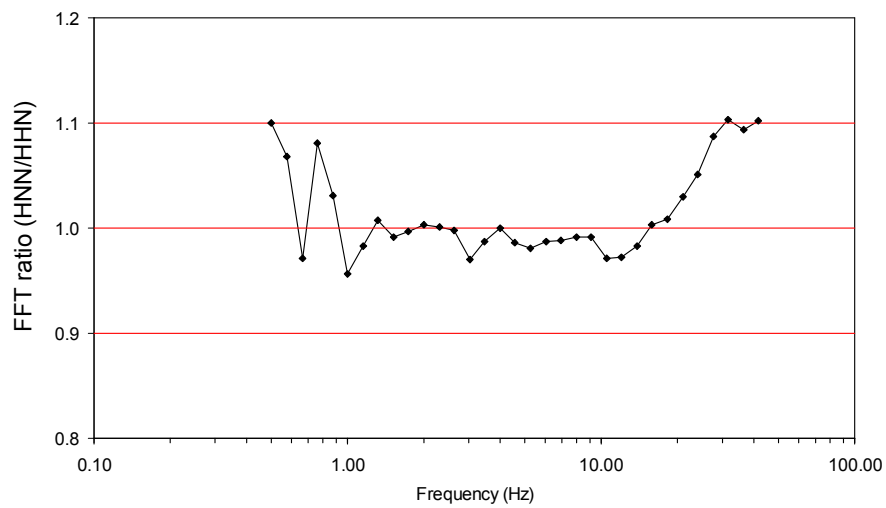


Figure 8. Fourier amplitude ratio of HNN/HHN (log-log scale).